Available online at www.sciencedirect.com
ScienceDirect
Coordination Chemistry Reviews 252 (2008) 2137–2154
COORDINATION CHEMISTRY REVIEWS
www.elsevier.com/locate/ccr

Review

Groups 3 and 4 single-site catalysts for styrene–ethylene and styrene–α-olefin copolymerization

Anne-Sophie Rodrigues, Jean-François Carpentier*

Catalyse et organométalliques, UMR 6226 CNRS-Université de Rennes 1, 35042 Rennes Cedex, France

Received 28 September 2007; accepted 24 November 2007
Available online 3 December 2007

Contents

* Corresponding author. Tel.: +33 223 235 950; fax: +33 223 236 939.
E-mail address: jean-francois.carpentier@univ-rennes1.fr (J.-F. Carpentier).

0010-8545/$ – see front matter
doi:10.1016/j.ccr.2007.11.023

Abstract

Styrene–ethylene and styrene–α-olefin copolymers are relatively new materials that were developed since the early 1990s thanks to homogeneous single-site catalysts. A wide range of copolymers, differing in their compositions, microstructures and properties have been prepared by using several types of early transition (groups 3 and 4) metal catalysts, which are critically reviewed in this contribution. Structure–activity–control relationships are also discussed.

Keywords: Group 4 metals; Lanthanides; Polymerization catalysis; Styrene

1. Introduction

Copolymerization of different monomers generally leads to polymeric materials with unique properties that differ from those of the respective homopolymers or of homopolymers blends. Thus, transition metal-catalyzed copolymerization of olefins and dienes with the widespread styrene monomer has been extensively studied, though with rather modest results due to the very dissimilar nature of active species responsible for styrene and other monomer polymerization.

Heterogeneous Ziegler–Natta catalysts are not suitable for the synthesis of styrene–ethylene copolymers. Indeed, besides low activity, they only incorporate very small amounts of styrene (usually less than 1%), mainly as isolated units [1,2]. Furthermore, the obtained polymers are mixtures of homo- and copolymers, due to the different catalytic active centers that are present in those catalytic systems.

The development of homogeneous single-site catalysts led to a considerable expansion in the copolymerization field since the early 1990s. By proper design of the catalytic system, to eventually tackle the different reactivity of those monomers, and selection of the polymerization conditions, a variety of copolymers with different compositions, structures (block, alternated, random) and properties (thermoplastic or thermo-elastomeric materials) could be achieved [3,4]. We present in this review the different homogeneous catalyst types efficiently used for styrene–ethylene and styrene–α-olefin copolymerization, all of them are based on groups 3 and 4 metal complexes, with a focus on the microstructure and possible stereocontrol of the obtained copolymers. Structure–activity relationships, origins of the microstructure control and mechanisms are discussed.

2. Copolymer properties, applications and microstructure

2.1. Properties and applications of styrene–ethylene copolymers

The introduction of styrenic groups in the PE backbone results in drastic changes in the viscoelastic behavior and thermo-mechanical properties of the polymeric material [5]. For instance, the crystallizability of PE chains is gradually inhibited by the incorporation of styrene. Thus, depending on the styrene content, ethylene–styrene interpolymers (ESI, developed by Dow Chemicals, see Section 5) range from semi-crystalline to amorphous materials [6]. Their viscoelastic behavior has been studied [7,8], as well as their miscibility properties with PE and different copolymers with various styrene content [9]. Thus, they are effective blend compatibilizers for PS/PE blends. ESI polymers have also potential in foam, films and sheet applications. Their current range of markets and applications include bitumen modifier, packaging, injection- and blow-molded articles, adhesives, toys, wire and cables as well as automotive, building and construction [5,10].

2.2. Copolymer microstructure

Styrene–ethylene copolymers microstructure is accurately determined by ^{13}C NMR spectroscopy: each carbon in a different monomer sequence has a specific environment and thus a characteristic chemical shift. The convention used for assigning carbon labels was first described by Randall [11]. S stands for secondary (methylene) carbon and T stands for tertiary (methine) carbon. The Greek letters indicate the relative position of the nearest tertiary carbon in both directions along the polymer chain. Possible sequences are depicted in Fig. 1 and assignments reported in the literature are summarized in Table 1.

The presence of $S_{\alpha\beta}$ methylene carbons can arise from regio-irregular styrene–styrene sequence (primary insertion followed by secondary insertion) or styrene–ethylene–styrene sequence (secondary insertion followed by ethylene and primary insertion), as illustrated in Fig. 2. Regardless of their formation pathway, the presence of $S_{\alpha\beta}$ methylene carbons brings unequivocal evidences that styrene inserts both in a primary and secondary fashion since both sequences involve both types of styrene insertion. Likewise, it is not possible to discern whether $S_{\alpha\gamma}$ and $S_{\beta\gamma}$ carbons arise from primary insertion of styrene followed by two successive ethylene insertions and then secondary styrene insertion or secondary insertion of styrene followed by ethylene and then primary insertion.

The copolymer microstructure is mainly controlled by the nature of the catalytic system. Hence, different types of copoly-

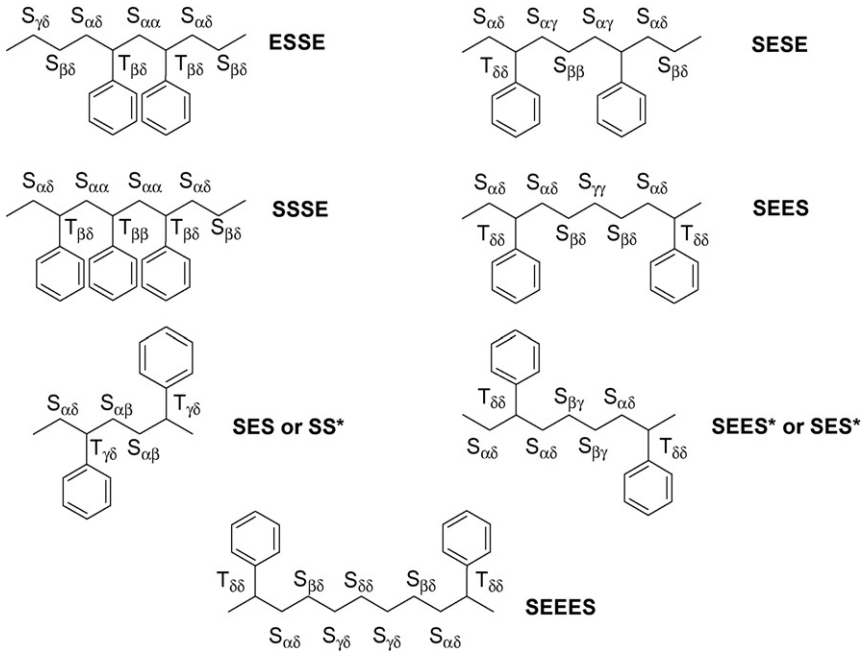

Fig. 1. Possible monomer sequences in styrene–ethylene copolymers.

mers were obtained using the catalytic systems described below.

3. Group 4 metallocene catalysts

3.1. Bridged cyclopentadienyl–fluorenyl catalysts

There have been some discrepancies among several authors concerning the catalytic performances of metallocenes in styrene–ethylene copolymerization and the resulting copolymer microstructure and properties. For instance, using $(C_5H_4CMe_2Flu)ZrCl_2$ (**1**, Fig. 3) (Flu = 9-fluorenyl) activated by MAO (650 equiv.), Ren obtained a copolymer with a styrene content of 10 mol% and a high molecular weight (M_n = 100,000 g/mol), presenting isolated styrene units and styrene–ethylene–styrene (SES) sequences in a head-to-tail configuration [12].

On the other hand, Kaminsky achieved higher molecular weights (M_n up to 400,000 g/mol) and higher styrene incorporation (up to 38 mol%) using the same catalyst or substituted

Table 1
^{13}C NMR assignments for styrene–ethylene copolymers

Sequence	Carbon	δ (ppm from TMS)
E*S*SE	$S_{\alpha\alpha}$	43.3–44.0
S*S*SE	$S_{\alpha\alpha}$	44.3
S*S*SS	$S_{\alpha\alpha}$	44.5–44.7
*S*S* or S*E*S*	$S_{\alpha\beta}$	34.3–34.7; 35.1–35.8
S*E*S	$S_{\alpha\gamma}$	35.0–37.0
E*S*E	$S_{\alpha\delta}$	36.7–37.0
ES*S*E	$S_{\alpha\delta}$	37.9
SS*S*E	$S_{\alpha\delta}$	37.4
S*E*S	$S_{\alpha\delta}$	25.2–25.4; 36
S*E*S	$S_{\beta\beta}$	24.8–25.6
S*EE*S or S*E*S*	$S_{\beta\gamma}$	27.5
S*EE*S	$S_{\beta\delta}$	27.0–27.8
SE*E*S	$S_{\gamma\gamma}$	29.7–29.9
SE*E*ES	$S_{\gamma\delta}$	29.4–30.3
SE*E*ES or EEEEE	$S_{\delta\delta}$	29.7–30.0
S*S*SE	$T_{\beta\beta}$	41.0–41.4
S*S*SS	$T_{\beta\beta}$	40.6–40.9; 45.4
ES*S*E	$T_{\beta\delta}$	43.4–43.5
SS*S*E	$T_{\beta\delta}$	42.5–43.7
SE*S*S* or S*S**ES	$T_{\gamma\gamma}$	45.2–46.7
*S*E*S* or *S*S**	$T_{\gamma\delta}$	45.2–46.7
EE*S*EE or *S*EE*S* or *S*E*S*	$T_{\delta\delta}$	45.0–46.7

S* indicates regioirregular styrene insertion.

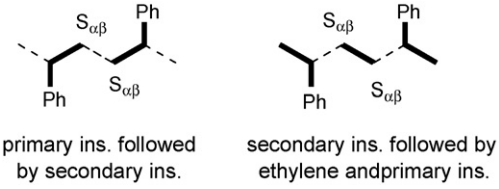

Fig. 2. Possible formation pathways of $S_{\alpha\beta}$ methylene carbons.

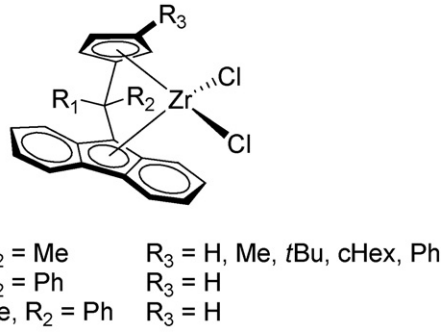

Fig. 3. Bridged Cp–Flu zirconocene catalysts precursors used for styrene–ethylene copolymerization [12–16].

Table 2
Styrene–ethylene copolymerization with catalyst precursors **1–7**

Catalyst system	T_p (°C)	Maximum % St incorporation (mol%)	Microstructure (observed sequences)	M_n ($\times 10^{-3}$ g/mol)	M_w/M_n	Reference
1/MAO	40	10	Pseudo-random (EESEE, SES)	100	nr	[12]
1/MAO	30	6	nr	324–423	2.2–3.2	[15]
1/MAO	30	37	nr	77–340	nr	[13]
2/MAO	30	29	nr	26–253	nr	[13]
3/MAO	30	5	nr	101–270	nr	[13]
4/MAO	30	16	nr	101–292	nr	[13]
5/MAO	30	38	nr	96–422	nr	[13]
6/MAO	30	27	nr	92–363	nr	[14]
7/$AlMe_3$	50	34	Pseudo-random (SEEES, SEES, SES* or SS*)	nr	nr	[16]

nr: not reported.

analogues [13]. Alkyl substituted systems (**2–4**) activated by MAO ([MAO]/[Zr] not reported) led to a decrease in both styrene incorporation and molecular weights with increasing steric hindrance, while the systems based on the phenyl substituted complex (**5**) could enhance catalytic activities and molecular weights, probably due to an electronic effect that compensates the steric crowding. The more sterically hindered complex **6** that has phenyl substituents on the bridge allowed a somewhat lower styrene insertion but led to higher molecular weights compared to complex **1** (Table 2) [14].

Zambelli and co-workers also investigated the regiospecificity of styrene insertion with a closely related system $\{C_5H_4C(Me)(Ph)Flu\}ZrCl_2$ (**7**) activated by $Al(^{13}CH_3)_3$ (150 equiv.) and found that secondary styrene insertion is prevailing, at least in the initiation step [16]. The copolymers obtained showed 32–34 mol% incorporated styrene, with the presence of SEEES, SEES and SES sequences (ethylene unit bridging head-to-head arranged styrene units) and/or SS sequences (tail-to-tail configuration), *i.e.* regio-irregular styrene insertion [16].

More recently, another catalytic behavior for the system **1**/MAO (2000 equiv. of MAO) was described: Martínez-Salazar reported that this catalyst led to a heterogeneous mixture of homopolyethylene or of two ethylene–styrene copolymers with different styrene contents, as determined by DSC [15]. Furthermore, the maximum styrene content achieved was quite low (6 mol%), *i.e.* comparable to the one first reported by Ren.

3.2. Bridged bis(indenyl) catalysts

C_2-symmetric complexes were also used with the hope of achieving copolymers with stereoregular styrene sequences. Oliva and co-workers first reported the synthesis of alternated stereoregular styrene–ethylene copolymers (for a styrene content of ca. 44 mol% in the copolymer) with *rac*-(EBI)$ZrCl_2$ (**9**, Fig. 4) (EBI = 1,2-ethylenebis(indenyl)) activated by MAO (100 equiv.) at low polymerization temperature (below 0 °C) [17]. This copolymer was crystalline and was characterized by ^{13}C NMR spectroscopy and wide-angle X-ray diffraction (WAXS) [18]. The ^{13}C NMR spectra were in good agreement with that of model polymers prepared by hydrogenation of poly(phenylbutadiene) [19] and low molecular mass compounds such as 2,7-diphenylnonane [20].

A very similar material was obtained with a system based on the single-carbon-atom bridged *rac*-(isopropylidene)bis(indenyl) zirconocene (**10**). The recovered copolymer was stretchable and could be oriented, allowing a complete X-ray diffraction analysis [21]. The latter analysis confirmed the isotactic stereochemical configuration of the

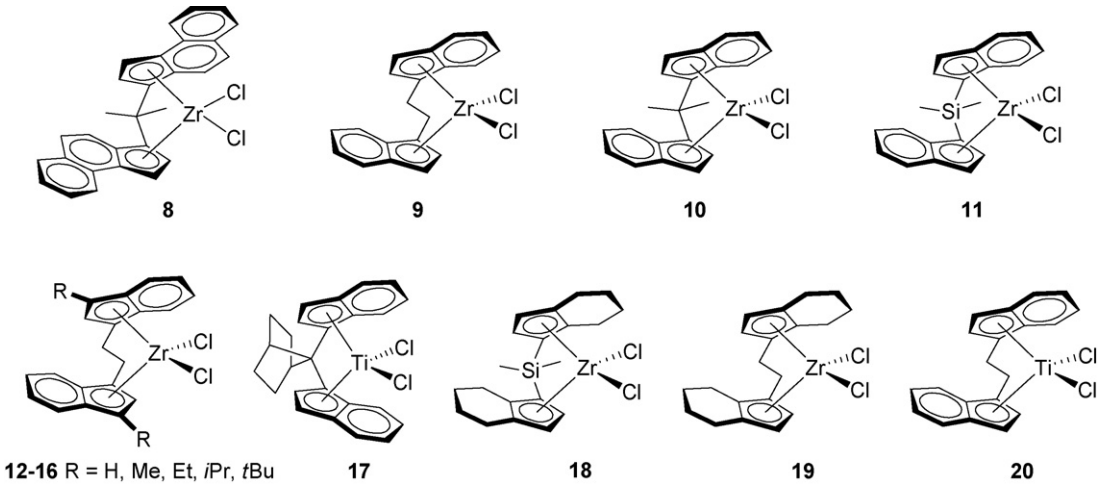

Fig. 4. Bridged bis(indenyl) group 4 catalyst precursors used for styrene–ethylene copolymerization [14,15,17,21–27].

styrene units relative to the polymer chain and hence the previous NMR assignments. The monomer alternation was attributed to the inability of the catalysts to give styrene–styrene sequences and to a penultimate effect, *i.e.* styrene insertion is preferred when the penultimate inserted monomer unit is a styrene one [22].

Arai and co-workers also reported the formation of stereoregular copolymers (head-to-tail styrene sequences and isotactic structure), using catalyst precursors **9**, **10** and **8** activated by MAO at higher polymerization temperature ($T_p = 50\,^{\circ}C$), but with a *random* styrene incorporation (10–52 mol%) [23,24]. Compared with its ethylene-bridged analogue **9**, isopropylidene-bridged pre-catalyst **10** showed higher productivity and styrene incorporation ability and afforded copolymers with higher molecular weights ($M_n \approx 80{,}000$ g/mol vs. 25,000 g/mol) [24]. Unexpectedly, the sterically hindered complex **8** showed a strikingly better reactivity towards styrene, offering copolymers with styrene content as high as 73 mol% (this complex was also reported as an isospecific styrene polymerization catalyst [23]). The isotacticity (of SSS and SES sequences) was independent of the styrene content for both catalysts **10** and **8**, which led the authors to speculate on a site stereocontrol mechanism [23].

Likewise, Kaminsky observed a similar relationship between the catalyst bite angle and its styrene incorporation ability. Indeed, the silylene-bridged complex **11** could only incorporate 5 mol% of styrene while under the exact same conditions, isopropylidene-bridged complex **10** led to a styrene content of 41 mol% [14]. The assumption of the bite angle impact (on steric grounds) was also supported by the fact that higher molecular weight copolymers were obtained with **11** than with **10**: the sterically demanding β-H elimination occurs with greater ease at the more open geometry of the isopropylidene-bridged metallocenes [14].

Surprisingly, the introduction of a bulky substituent such as a *tert*-butyl group in the 3-position of the indenyl ligand drastically modifies the catalytic behavior of the complex (**16**), leading to a *block* copolymer having long polyethylene and isotactic polystyrene crystalline sequences that arrange themselves into two distinct crystalline lattices, as determined by ^{13}C NMR, DSC and WAXS [25]. The peculiarity of this catalyst behavior was attributed to an unusual primary styrene insertion and the fact that the aromatic ring of the last inserted unit interacts with the metal center. Noteworthy, this type of block copolymer had not been prepared at that time with homogeneous group 4 catalysts before. Rather, an indirect synthetic strategy employing hydrogenation of block styrene–butadiene copolymers was used [28].

The effect of the substituent in the 3-position on insertion regio- and stereochemistry was further scrutinized [26]. For R = H, Me and Et (**12**–**14**), styrene insertion is mainly secondary, giving *pseudo*-random copolymers with alternating SES sequences but without stereoregularity while for R = *i*Pr or *t*Bu (**15**–**16**), primary insertion prevails and thus decreases the tendency of alternating enchainment of ethylene and styrene. Furthermore, the stereocontrol changes from isotactic-like to syndiotactic-like with R = Et and *i*Pr. This phenomenon was proposed to be possibly induced by an asymmetric carbon induction that overcomes the isotactic-like stereocontrol expected from the C_2-symmetric catalytic center. By further increasing the steric hindrance (R = *t*Bu), the catalyst site control is restored [26].

More recently, the synthesis of the stereorigid *meso*-[norbornane-7,7-bis(indenyl)]titanium chloride (**17**) was described and, when activated with MAO, this catalyst was claimed to show high activity in styrene–ethylene copolymerization, yielding copolymers with unprecedented homogeneous chemical compositions [27]. It was suggested that the inclusion of the bicycle hinders the rotation of the bridge carbon atom-indenyl bonds, resulting in a remarkable conformational stability that remains fixed all along the catalytic process. Consequently, the activity of the catalyst system based on **17** is considerably higher than that observed with other *ansa*-metallocenes (Zr and Ti). This would indicate that the activity is mainly controlled by geometrical factors and not by the nature of the metal center. However, the obtained copolymers show quite modest styrene incorporation (4 mol%) but high molecular weights (M_n up to 171,000 g/mol), and the chemical composition profiles determined by crystallization–fractionation analysis are all unimodal and extremely narrow.

The latter result is in striking contrast with previous results which indicated that titanium-based metallocenes (**20**) are rather ineffective catalyst precursors for styrene–ethylene copolymerization, giving only small amounts of PE [15].

On the other hand, the catalyst systems based on bridged bis(tetrahydroindenyl) zirconocenes **18** and **19** were more stable than their indenyl counterpart, possibly because decomposition by ring-slippage cannot occur. Thus, polymers with higher

Table 3
Styrene–ethylene copolymerization catalyzed by C_2-symmetric group 4 metallocenes

Catalyst precursor	T_p (°C)	Maximum % St incorporation (mol%)	Microstructure (observed sequences)	M_n ($\times 10^{-3}$ g/mol)	M_w/M_n	Reference
8	50	73	Random (SSS, EESEE, ESES, ESSE, SSES)	27	1.9	[23]
9	<0	44	Alternated (SESE)	nr	nr	[17,18]
9	50	9	Random (EE, ESES, SSS)	25	2.0	[24]
10	50	52	Random (EE, ESES, SSS)	80	2.1	[24]
15	20	28	Block (SSS, EEE, SSEE, EESEE)	5	2.0	[25]
17	35	4	nr	171	1.9	[27]
18	35	0.4	nr	189	1.9	[15]
19	35	1	nr	59	1.9	[15]

nr: not reported.

molecular weight (M_n up to 189,000 g/mol) were obtained and styrene incorporation followed the same trend as previously observed when varying the nature of the bridge (Table 3) [15].

4. Group 4 metal half-sandwich complexes

The success of titanium half-sandwich catalysts to promote syndiospecific styrene polymerization reported in the mid-1980s naturally led to some investigations of these catalytic systems for styrene–ethylene copolymerization. However, this type of complex often gives homopolymers as by-products, requiring tedious fractionation steps to recover the desired copolymer material.

4.1. $CpTiCl_3$/MAO

This catalyst system gave rise to polemic statements from different laboratories. In an early paper, Longo reported that styrene–ethylene copolymers with syndiotactic sequences are obtained with $CpTiCl_3$/MAO and found that the copolymer microstructure and composition strongly depends on the [Al]/[Ti] ratio [29]. In particular, for an [Al]/[Ti] ratio of 1000, a block copolymer with syndiotactic styrene sequences bridged by ethylene units was claimed to be produced, while for a ratio of 100, the copolymer was supposed to contain isolated styrene units bridging polyethylene sequences. However, according to Aaltonen and Seppala, the same catalytic system afforded only a mixture of PE and sPS, even under closely similar conditions [30,31]. This latter result was denied and further contributions claiming the formation of copolymers (styrene content ranging from 27 to 36 mol%) were reported [18,32]. It was stated that the $CpTiCl_3$/MAO system is very sensitive to the reaction conditions, including the exact mixing sequence and pre-contacting time, which usually leads to poor reproducibility. A point that the authors failed to underline is that a difference in the MAO-type (*i.e.* residual $AlMe_3$ content) used to activate this catalyst might also have a major impact, as observed with other catalytic systems.

More recently, the production of a sPS–PE block copolymer was claimed, still with the same catalytic system $CpTiCl_3$/MAO, using a sequential monomer feed scheme [33]. However, the characterization of the material obtained was not conclusive since both NMR and thermal analyses of long block structures show results that would be identical for mixture of homopolymers. The slight difference in the crystallization behavior between the sample and homopolymers blend does not seem very convincing either, given that "intimate" blends could also induce minor variations compared to "crude" blends, due to the fine level of dispersion achieved by *in situ* polymerization.

4.2. $Cp^*TiR_3/B(C_6F_5)_3$

Further to the controversy about the $CpTiCl_3$/MAO copolymerization capability, Pellecchia and Zambelli turned toward MAO-free catalytic systems, such as $Cp^*TiBz_3/B(C_6F_5)_3$ that proved extremely active for homopolymerization of both monomers and appears simpler and better characterized. Styrene–ethylene copolymerization mediated by this discrete catalyst led, for temperature above 50 °C and independently from the feed composition, to an almost perfectly alternating atactic copolymer (determined by ^{13}C NMR), together with some PE and sPS homopolymers (separated by fractionation) [34].

The regiospecificity was investigated by the use of ^{13}C-enriched $AlMe_3$ and secondary styrene insertion largely prevails over primary insertion in the initiation step. This led the authors to speculate on benzyl coordination of the growing chain, similar to previous suggestions for styrene homopolymerization [35]. Thus, the tendency of this catalyst to incorporate alternatively the two monomers could be attributed to the bonding mode of the last inserted monomer unit (η^1 for ethylene, η^n for styrene with $n \geq 2$). Consequently, the competitive monomer coordination would be affected: styrene coordination would be preferred over ethylene for the coordinatively unsaturated $Cp^*Ti–CH_2CH_2–Pol$ propagating complex (Pol = growing polymer chain), while ethylene would compete favorably for coordination to the more sterically hindered and less coordinatively unsaturated $Cp^*Ti(\eta^n–CH(Ph)CH_2–Pol)$ species.

Unexpectedly, the use of the closely related catalyst $Cp^*TiMe_3/B(C_6F_5)_3$ afforded polyethylene with ca. 3–5 mol% of 4-phenylbutyl branches [36]. This surprising result was ascribed to the multi-site nature of the catalytic system, containing a catalytic species able to cross-dimerize ethylene and styrene to 6-phenyl-1-hexene [identified in the polymerization mixture] and another species able to copolymerize the latter with ethylene. The detailed analysis of the oligomeric fraction by GC–MS and NMR led the authors to propose a mechanism involving Ti^{II} active species and metallacycle intermediates to explain the observed selectivity in co-oligomerization (Scheme 1) [37].

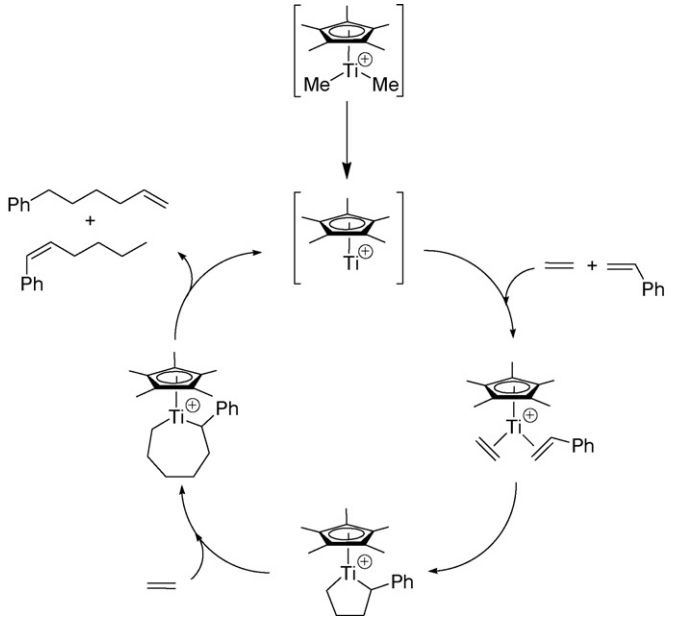

Scheme 1. Proposed mechanism for the formation of phenyl-1-hexenes with $Cp^*TiMe_3/B(C_6F_5)_3$ [36,37].

4.3. $CpTi(OR)_3$/MAO

Other titanium half-sandwich catalysts, such as $CpTi(OPh)_3$/MAO were investigated for styrene–ethylene copolymerization [38]. This system exhibits a quite good catalytic activity (up to 100 kg/(mol_{Ti} h)) and gives an amorphous elastoplastic copolymer presenting a random microstructure. A styrene content of 55 mol% could be achieved under relatively mild polymerization conditions (toluene, 60 °C, 1 atm ethylene, MAO/Ti = 600). The copolymer microstructure, composition and molecular weight were strongly dependent upon the polymerization conditions: co-monomer feed ratio, polymerization temperature, [Al]/[Ti] ratio and TMA content in MAO: for [Al]/[Ti] < 1000, the copolymerization product was essentially random E–S copolymer while for [Al]/[Ti] > 1000, mainly sPS was obtained. A TMA content in MAO above 30 mol% was detrimental for obtaining styrene–ethylene copolymer in favor of sPS.

ESR investigations suggested that PE is produced by a cationic Ti^{IV} active center, sPS by a Ti^{III} species and a third intermediate complex was postulated for the copolymerization of styrene with ethylene.

The microstructure of the copolymer was determined by ^{13}C NMR which revealed isolated styrene units ESE together with SEE, SES and SES*, *i.e.* ethylene unit bridging head-to-head styrene arrangement (*i.e.* regio-irregular insertion). For relatively higher styrene concentration (44 mol%), SSE and ESSE sequences were found in addition to the previously observed sequences.

Very similar results were obtained with the congener catalytic system $Cp^*Ti(OBz)_3$/MAO: after fractionation, an elastoplastic copolymer was recovered with some PE and PS [39,40]. Its structure and composition were dependent on polymerization conditions, especially the [Al]/[Ti] ratio and TMA content of the MAO. The same type of random microstructure was observed [39,40].

4.4. $Cp'TiCl_2X$/MAO (X = aryloxide, ketimide)

Modified titanium half-sandwich catalysts, in which one of the chloride ligand was replaced by another anionic ligand X, either an aryloxide (complexes **21**–**31**, Fig. 5) or a ketimide group (complexes **33**–**35**), were reported to be efficient catalysts for styrene–ethylene copolymerization [41–43].

Contrasting with previous observations when using other titanium half-sandwich catalytic systems, only negligible amounts of PE and PS were formed during styrene–ethylene copolymerization. In other words, it was considered that copolymers were obtained exclusively. The substitution patterns of the cyclopentadienyl ligand directly affected catalytic activity and copolymer molecular weight: complex **31** showed the poorest activity (740 kg/(mol_{Ti} h)), indicating that the global steric bulk (when considering internal rotation of the cyclopentadienyl group) had a high impact on activity. The obtained copolymers presented relatively high molecular weights (M_n = 15,000–106,000 g/mol) with narrow polydispersities (M_w/M_n = 1.6–2.2) and relatively high incorporated styrene contents (25–74 mol%) at high [styrene]/[ethylene] ratio in the feed [41,42].

The ^{13}C NMR analysis of the copolymers revealed the presence of tail-to-tail, SES or head-to-head styrene sequences together with atactic head-to-tail styrene connections. The Cp substituents also had an influence on the regioselectivity observed: copolymers obtained with *tert*-butyl-substituted complex **23** showed the lowest regioselective SS linkage, as determined by the value of $[S_{\alpha\beta}]/[S_{\alpha\alpha} + S_{\beta\beta}]$ ratio ($[S_{\alpha\beta}]/[S_{\alpha\alpha} + S_{\beta\beta}] = 2.94$) while the more hindered complex **32** exhibited rather good regioselectivity ($[S_{\alpha\beta}]/[S_{\alpha\alpha} + S_{\beta\beta}] = 1.12$) [42].

Consistent with other literature reports, the authors suggested the possible existence of several catalytic species (multi-site behavior), one being active for syndiospecific styrene polymerization and another one for styrene–ethylene copolymerization, postulated as a cationic Ti^{IV} species of the type $[CpTiLR]^+$. Rather convincing evidence was brought by stepwise copolymerizations: the active species for styrene homopolymerization (Ti^{III} species) seems to be tuned *in situ* upon oxidation by ethylene addition and it appeared that once formed, these catalytic active species could not be converted again to perform styrene polymerization after ethylene removal [43]. However, further mechanistic studies, *e.g.* ESR measurements of Ti^{III} and Ti^{IV} species, seem necessary to confirm this hypothesis.

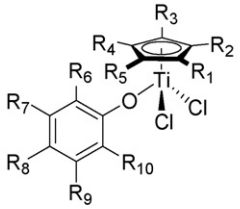

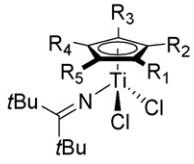

21-22	$R_{1\text{-}5}$ = H, Me	$R_6 = R_{10}$ = *i*Pr, $R_{7\text{-}9}$ = H
23	R_1 = *t*Bu $R_{2\text{-}5}$ = H	$R_6 = R_{10}$ = *i*Pr, $R_{7\text{-}9}$ = H
24-25	$R_1 = R_3$ = Me, $R_{2,4,5}$ = H	$R_6 = R_{10}$ = *i*Pr, Me, $R_{7\text{-}9}$ = H
26-28	$R_1 = R_3$ = *t*Bu, $R_{2,4,5}$ = H	$R_6 = R_{10}$ = *i*Pr, Me, *t*Bu, $R_{7\text{-}9}$ = H
29-30	$R_1 = R_3$ = *t*Bu, $R_{2,4,5}$ = H	$R_6 = R_8 = R_{10}$ = Me, *t*Bu, $R_{7,9}$ = H
31	$R_1 = R_3 = R_5$ = Me, $R_{2,4}$ = H	$R_6 = R_{10}$ = *i*Pr, $R_{7\text{-}9}$ = H
32	$R_1 = R_2 = R_3$ = Me, $R_{4,5}$ = H	$R_6 = R_{10}$ = *i*Pr, $R_{7\text{-}9}$ = H

33-34	$R_{1\text{-}5}$ = H, Me
35	R_1 = *t*Bu $R_{2\text{-}5}$ = H

Fig. 5. Aryloxide and ketimide titanium half-sandwich catalyst precursors used for styrene–ethylene copolymerization [41–45].

Living styrene–ethylene copolymerization was first achieved with ketimide titanium half-sandwich catalysts Cp*$TiCl_2$(N = C*t*Bu_2) (**34**, Fig. 5) [44,45]. A linear relationship between the molecular weights and the yields was observed while the molecular weight distributions remained narrow ($M_w/M_n \approx 1.1$–1.6). However, styrene incorporation was slightly lower than with the aryloxide complexes, reaching a maximum of 15 mol% and no significant differences in the styrene content were observed over time course. Consequently, no styrene repeating units were observed. Noteworthy, complex **33** featuring a non-substituted Cp ligand was inactive towards copolymerization, revealing that steric and electronic features of this ligand strongly influence styrene incorporation, similar to what was observed with aryloxide complexes [44]. The living behavior was maintained over a wide range of polymerization conditions ([Al]/[Ti] molar ratio = 500–3000, T_p = 25–40 °C, 4–6 atm ethylene, [styrene] = 1.45–4.35 mol/L) [45].

4.5. Zirconium and hafnium half-sandwich catalysts

Contrasting with their titanium counterparts, zirconium and hafnium half-sandwich catalysts were generally inactive towards both styrene homo- and copolymerization with ethylene. However, a recent contribution reported that MAO-activated Zr and Hf systems which incorporated a phosphorus-pendant Cp ligand (complexes **36**–**39**, Fig. 6) showed modest activity for ethylene and styrene–ethylene copolymerization (up to 110 kg/(mol_M h) at 80 °C) [46]. The obtained copolymers presented relatively high styrene incorporation (31–87 mol%) and molecular weights (M_n = 6000–20,000 g/mol) but very broad polydispersities (M_w/M_n = 4.6–19.3), a feature that points out a likely multi-site character of this catalyst system [46].

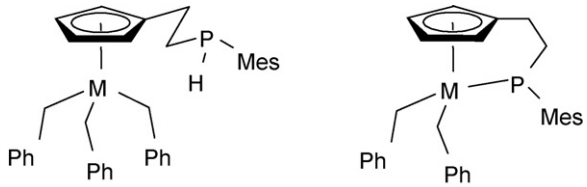

36 M = Zr
37 M=Hf
38 M = Zr
39 M=Hf

Fig. 6. Zirconium and hafnium half-sandwich catalyst precursors incorporating phosphorus-pendant ligand used for styrene–ethylene copolymerization [46].

5. Constrained geometry catalysts (CGCs)

The development of styrene–ethylene copolymers gained renewed interest with the so-called "constrained geometry" catalysts (CGCs) (Fig. 7) [47,48]. The synthesis of those complexes was first described by Bercaw and co-workers [49,50] and Okuda et al. [51,52]. Soon after, applications of such Ti–CGC catalysts for olefin (co)polymerization appeared in the patent literature [53,54]. Consequently to the inability of these complexes to homopolymerize styrene, no polystyrene impurities are formed during styrene–ethylene copolymerization.

Dow Chemicals reported copolymers with styrene content up to 48 mol%. The microstructure of those copolymers shows only tail-to-tail styrene–styrene sequences. Hence, the maximum theoretical styrene content is about 50 mol%. Furthermore, styrene incorporation was regio- and stereoirregular. Consequently, these copolymers are defined as "*pseudo*-random", *i.e.* without sequential head-to-tail styrene insertions and with monomer distribution that is otherwise random or nearly so [53]. These so-called "ethylene–styrene interpolymers" (ESI) display a unique set of physical characteristics, from crystalline thermoplastics to amorphous elastomers, also called "glasstomers" (*vide supra*) [10].

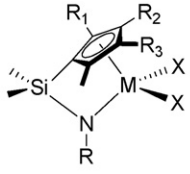

40-46	M = Ti	X = Cl	R_1 = Me	$R_2 = R_3$ = Me	R = *t*Bu, Bz, Ph, C_6F_5, SO_2Ph, SO_2Me, Cy
47	M = Ti	X = Me	R_1 = Me	$R_2 = R_3$ = Me	R = *t*Bu
48	M = Zr	X = *i*Bu	R_1 = Me	$R_2 = R_3$ = Me	R = *t*Bu
49-52	M = Ti	X = Cl	R_1 = H, Bu, Ph, C_6H_4F	$R_2 = R_3$ = Me	R = *t*Bu
53	M = Ti	X = Me	R_1 = H	$R_2 = R_3$ = Ph	R = *t*Bu

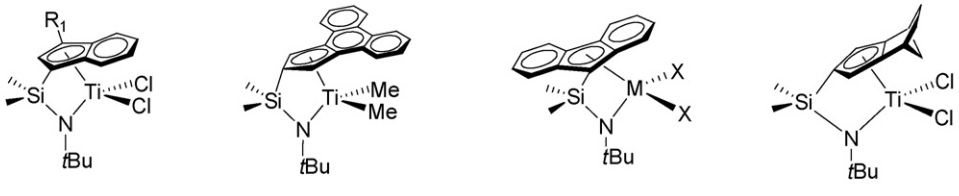

54-55 R_1 = H, $SiMe_3$
56
57 M = Zr X = Cl
58 M = Ti X = Me
59

Fig. 7. Constrained geometry group 4 catalyst precursors used for styrene–ethylene copolymerization [53,55–63].

5.1. Influence of polymerization conditions

In order to establish some catalyst structure/copolymer properties correlation, Mülhaupt and Waymouth systematically studied the influence of copolymerization conditions on copolymer composition and microstructure with pre-catalyst **40**, activated with 2000 equiv. of MAO [56]. As previously observed with other systems, increasing styrene concentration in the monomer feed lowered both catalytic activity and polymer molecular weight, and a linear relationship between styrene concentration in the feed and incorporated styrene in the copolymer was found only at low styrene content. This is assumed to result from increased catalytic deactivation by coordination of the phenyl ring of the last 2,1-inserted styrene unit and an increased of chain-transfer rate following styrene insertion. The reactivity ratios ($r_E = 23.4$ and $r_S = 0.015$) calculated from a Fineman–Ross plot [64] revealed a clear preference for ethylene multiple insertion. ^{13}C NMR investigations showed only resonances for tail-to-tail coupling SS sequences (or SES sequence) and PE sequences; in other words, no more than two styrene units follow each other. Melting and glass transition temperatures (T_m and T_g) of the copolymers are strongly affected by the styrene content: with increasing styrene content, a pronounced decrease of T_m and increase of T_g was observed.

5.2. Influence of the C_5R_4 ligand

The effect of ligand substitution on styrene–ethylene copolymerization behavior was probed by comparing the catalytic performances of complexes **40**, **41**, **54**, **55**, **57** (Table 4) [57]. High electron density at the Cp ring and at the amide function accounts for higher activity, while less electron-donating or electron-withdrawing substituents tend to lower catalytic activity (**40** (Cp*) > **54** (Ind) > **55** (3-SiMe$_3$-Ind) and **40** (N*t*Bu) > **41** (NBz)). Bulky substituents on the C_5R_4-ligand result in steric hindrance and thus reduce styrene incorporation (only 1.1 mol% incorporated styrene with fluorenyl complex **57** compared to 15.8 mol% with Cp* **40**) but increase the long-term activity of the catalyst. Significantly higher molecular weights were obtained with fluorenyl complex **57**, likely due to a reduced β-H elimination rate.

Xu detailed the styrene–ethylene copolymerization behavior of the closely related discrete cationic complex [(Me$_2$SiFluN*t*Bu)TiMe]$^+$[B(C$_6$F$_5$)$_4$]$^-$ (**58**) [58]. This catalyst yielded exclusively PE at 0 °C but afforded predominantly styrene–ethylene copolymer at 50 °C as determined by solvent fractionation. The copolymer microstructure was analyzed by ^{13}C NMR and surprisingly, an almost perfectly alternating structure with well-defined isotactic styrene arrangement was found: resonances assigned to $S_{\beta\beta}$ (SES sequences), $S_{\alpha\beta}$ (SES) and $T_{\delta\delta}$ (ESE) in a 1:2:1 ratio. Furthermore, comparison of those samples with Suzuki's assignments for hydrogenated 1,4-polyphenylbutadiene [19] suggests the only presence of *m* diads and *mm* triads along the polymer backbone. This peculiar microstructure, as well as the copolymer composition, was independent of the monomer feed, reaction temperature and addition of TIBA or MAO (as scavengers). The monomer and stereocontrol insertion are proposed to come from repulsive steric interactions that reinforce monomer orientation and a systematic interconversion of the active site after each monomer insertion, in analogy with syndiospecific propene polymerization with (C$_5$H$_4$CMe$_2$Flu)ZrCl$_2$/MAO [65,66].

An alternating tendency was also observed with (Me$_2$SiC$_5$Me$_4$*N*t*Bu)TiMe$_2$/[Ph$_3$C][B(C$_6$F$_5$)$_4$] (**47**) as illustrated by the reactivity ratios ($r_E = 9$, $r_S = 0.04$ and $r_E r_S = 0.4$; the theoretical value for a perfectly alternated copolymer is $r_1 = r_2 = r_1 r_2 = 0$ [67]) and ^{13}C NMR analysis that showed SES sequences, even at low styrene content. The ratio [$T_{\delta\delta}$]/[$S_{\beta\beta}$] was used to estimate the content of isolated styrene units ([$T_{\delta\delta}$]/[$S_{\beta\beta}$] = 2($n_{isolated}/n_{SES}$ + 1). For a copolymer presenting 14 mol% incorporated styrene, this value was 2.25, corresponding to 10 mol% of styrene as isolated units and 90 mol% as SES sequences [59].

These results are in striking contrast with the *pseudo*-random copolymer microstructure previously observed with MAO-activated CGC complexes [56,57]. The counterion coordination might thus play a significant role in the catalyst copolymerization behavior.

Further studies confirmed the fact that higher electron density on the cyclopentadienyl ligand results in enhanced activity: complexes **51**–**52** featuring less electron-donating and bulkier groups were one order of magnitude less active than their alkyl analogues **40**, **49**, **50** [60]. Styrene incorporation rate and polymer molecular weights were also affected. In addition, complex **59** was 30–60 times less active than **54** [61]. Thus, electron-donating groups with low steric congestion are required to obtain

Table 4
Styrene–ethylene copolymerization using different constrained-geometry catalyst precursors[a] [57]

Complex	Activity	Styrene content (mol%)[b]	M_n ($\times 10^{-3}$ g/mol)[c]	M_w/M_n[c]	T_g[d]	T_m[d]
40	3,074	15.8	51	2.2	−9.4	–
54	435	20.5	11	2.9	–	118.0
55	255	5.7	38	2.2	–	92.9
57	194	1.1	121	3.1	–	124.0
41	38	26.0	12	3.5	−2.2	122.7

[a] Polymerization conditions: [Catalyst] = 20 μmol/L, MAO/Ti = 2,000, [St] = 1.1 mol/L, [Et] = 0.22 mol/L, [St]/[Et] = 5:1 (mol), toluene, total volume = 200 mL, time = 1 h, T_p = 60 °C.
[b] Determined by ^1H NMR.
[c] Determined by GPC vs. PE standards.
[d] Determined by DSC.

good catalytic activity and styrene incorporation. This point was recently illustrated with complexes **53** and **56** that exhibit higher activity than **40** and relatively higher styrene incorporation under the same polymerization conditions (21.5 and 30.6 mol% vs. 11 mol% incorporated styrene content) [55].

5.3. Influence of the amido ligand

The importance of the donor properties of the amido-ligand on styrene–ethylene copolymerization performances was highlighted by the introduction of electron-withdrawing groups (Ph, C_6F_5, SO_2Ph, SO_2Me) on the nitrogen atom (complexes **42**–**45**) [62]. X-ray analyses of complexes **43** and **44** revealed that the introduction of electron-withdrawing groups resulted in a significant lengthening of the Ti–N bonds relative to the *tert*-butylamido complex **40**. Consequently, the metal center is more electron-deficient, which may account for the very poor productivities for styrene–ethylene copolymerization. Rather, those catalysts are up to 30 times more active for styrene homopolymerization, yielding predominantly sPS. Thus, the high ethylene homopolymerization activity and the low reactivity towards styrene of the CGC complexes is not a mere consequence of the steric constraint imposed by the Me_2Si-bridge, but also results from the strong donor behavior of the alkylamido ligand.

The steric bulk of this latter moiety is also crucial for styrene incorporation and copolymer microstructure. Indeed, Nomura showed that although the more sterically hindered complex **46** exhibits a somewhat lower activity, it offers a higher styrene incorporation ability than **40** and leads to an alternated copolymer [63].

5.4. Dinuclear complexes

In 2004, Marks described dinuclear constrained geometry catalysts (**60**, Fig. 8) that exhibit much better activity for styrene homopolymerization and can incorporate ca. 20% more styrene than its monometallic counterpart (*i.e.* up to 76 mol%) [68]. The unique catalyst structure of **60** induces a modification of regiochemistry enchainment: primary insertion competes with secondary insertion to a significant degree, as determined by ^{13}C NMR of PS samples. As a result, when styrene incorporation was >50 mol% in the copolymers, up to three head-to-tail coupled styrene units could be observed in addition to tail-to-tail diads usually observed with CGC systems.

This improved styrene incorporation ability was also observed for dinuclear catalysts featuring longer bridges (**61**–**63**) [69]. Noteworthy, the presence of a longer bridge between the two active sites contributes to enhance catalytic activity (**63** > **62** > **61**) but this more or less rules out multinuclear cooperative effects and underlines actually the major importance of the steric hindrance around the metal center.

6. Group 4 post-metallocenes

Non-cyclopentadienyl complexes have rarely been used for the preparation of styrene–ethylene copolymers. As a matter of fact, only two types of post-metallocene Ti complexes were reported to be active in styrene–ethylene polymerization, and conflicting results in the first case caused some controversies.

6.1. Bis(phenolate) complexes

Kakugo first mentioned that 2,2′-thiobis(6-*tert*-butyl-4-methylphenoxy)titanium dichloride (**68**, Fig. 9) activated by MAO affords, with modest activity, alternated isotactic styrene–ethylene copolymer along with sPS [70–72]. The authors concluded on two active species, one producing the copolymer and the other one producing syndiotactic polystyrene. Furthermore, the presence of sulfur atoms in the bridge was stated as crucial for styrene incorporation.

Those results were later refuted by Okuda, who demonstrated that also ethylene-bridged complexes (**65**–**66**) can incorporate styrene efficiently [73]. This was attributed to the more open coordination sphere around the metal center. The influence of the bridge, the X ligands as well as polymerization conditions (monomer and catalyst concentration) were examined in details [74]. The comparison of different ligand substituent patterns indicated that complexes allowing higher styrene incorporation

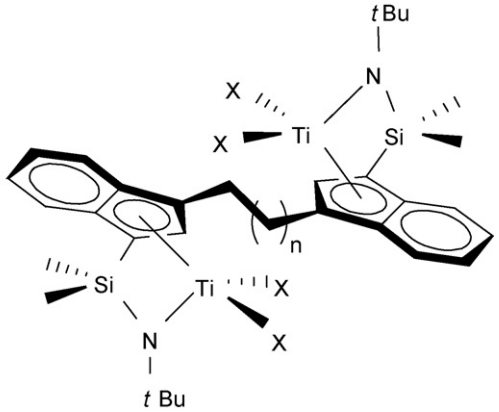

60	X = Me	n = 1
61-63	X = Cl	n = 5, 8, 11

Fig. 8. Dinuclear constrained geometry catalyst precursors used for styrene–ethylene copolymerization [68,69].

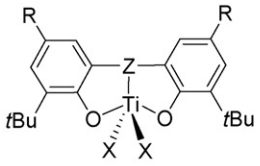

64	Z = CH_2	X = Cl	R = Me
65-67	Z = CH_2CH_2	X = Cl, O*i*Pr, Cp*	R = Me
68-70	Z = S	X = Cl, O*i*Pr, Cp*	R = Me
71-72	Z = S=O	X = Cl, O*i*Pr	R = Me
73-78	Z = $S(CH_2)_3S$	X = Cl, O*i*Pr	R = Me, *t*Bu, OMe

Fig. 9. Bis(phenolate) Ti catalyst precursors used for styrene–ethylene copolymerization [70–74].

(**65**, **66**, **71**) gave lower activities than complexes **64**, **68**, **69**, **72**. This was proposed to be due to both electronic and steric effects: for methylene and ethylene bridges, the eight- or nine-membered ring, consisting of the Ti, O and C atoms, adopts a boat conformation which allows a good π-donor O–Ti interaction that leads to a high electron density at the metal center and thus accounts for lower activity. In the case of the sulfur bridge, this latter enforces octahedral coordination, which results in an apparent increase of Lewis acidity and hence an increase of the activity. However, this latter situation also gives rise to a geometry presenting a good shielding of the Ti atom by the ligand, resulting in low styrene incorporation.

Increasing styrene concentration adversely affects both the catalytic activity and polymer molecular weights. On the other hand, styrene incorporation increases proportionally with styrene concentration but very high [styrene]/[ethylene] ratios (>85 mol%) are required to achieve significant, though still modest, styrene incorporation (>10 mol%). Furthermore, those catalysts rapidly deactivated after high initial activity, which might account for the observed heterogeneity of the copolymers chemical composition.

In contrast with Kakugo's results [70–72], no alternating styrene–ethylene microstructure was observed, even under very similar polymerization conditions. Instead, only ethylene blocks with isolated styrene units were detected. This observation was supported by the values found for the respective monomer reactivity ratios ($r_E = 111$ and $r_S = 0.055$). The formation of sPS was attributed to the extreme conditions (high styrene concentration, low ethylene pressure and prolonged reaction time) as well as the presence of MAO and undissolved complex that might be a source for alkoxy- and benzyl-titanium complexes, which were previously reported to promote syndiospecific styrene polymerization [75,76].

A slightly different behavior was observed with the 1,4-dithiabutanediyl-bridged complex **75**. Indeed, the copolymer microstructure could be varied by changing the monomers ratio in the feed and copolymers with styrene content up to 68 mol% were achieved [77]. For such copolymers (styrene content > 50 mol%), the presence of long isotactic styrene sequences occasionally interrupted by isolated ethylene units was evidenced by ^{13}C NMR. Styrene incorporation was also highly regiospecific (signals attributed to head-to-head and tail-to-tail styrene sequences were negligible). For copolymers with lower styrene content (<40 mol%), a more alternating tendency was observed, as illustrated by the SES sequences and isolated styrene units (EESEE). This latter point was confirmed by the values found for the Fineman–Ross copolymerization parameters ($r_E = 1.2$; $r_S = 0.031$ and $r_E r_S = 0.037$; the theoretical value for a perfectly alternated copolymer is given by $r_1 = r_2 = r_1 r_2 = 0$ [67]).

Styrene-rich copolymers (up to 99 mol% styrene content) with only few isolated ethylene units could also be achieved with this catalytic system when adding very small amounts of ethylene [78]. The ^{13}C NMR analyses of the styrenic units configuration in the vicinity of isolated ethylene unit allowed to determine that an enantiomorphic site control mechanism takes place rather than a chain-end controlled one.

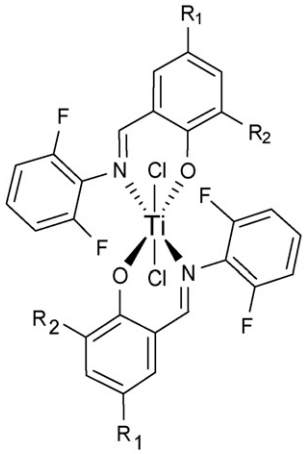

79 $R_1 = R_2 = I$
80-82 $R_1 = H$, $R_2 = t$Bu, $SiMe_3$, $C(CH_3)_2$-C_6H_5

Fig. 10. Phenoxy-imine Ti catalyst precursors used for styrene–ethylene block copolymerization [79].

6.2. Phenoxy-imine complexes

Recently, Weiser and Mülhaupt reported the synthesis of diblock styrene–ethylene copolymers by sequential monomer addition starting from PE block with phenoxy-imine Ti complexes (**79**–**82**, Fig. 10) [79]. Noteworthy, these complexes had never been reported for styrene polymerization before. High molecular weight copolymers were obtained (M_n up to 900,000 g/mol with **79**) with narrow polydispersity ($M_w/M_n = 1.2$–1.8) but poor styrene incorporation (up to 7.5 mol% with **81**) was achieved, even for high styrene concentration in the feed [79]. In addition, not all polyethylene chains initiated styrene block copolymerization. Consequently, a blend of the block copolymer and PE was obtained and, at high styrene concentrations, atactic polystyrene was also formed as a side product. Therefore, fractionation was required but PE proved difficult to separate from the block copolymer, leading to polymer blends forming micelles and phase separation of polymers with different morphology as observed by TEM [79].

7. Mechanistic insights

7.1. Active species

As in the case of syndiospecific styrene polymerization, the nature of the active species for styrene–ethylene copolymerization mediated by Ti-based catalysts is still strongly debated. Several authors have shown by ESR analyses that under polymerization conditions, tetravalent Ti^{IV} catalysts undergo reduction to Ti^{III} species [38,80,81]. Furthermore, it has been suggested that the cation $[CpTi^{III}R]^+$ is the active species for styrene homopolymerization, while a tetravalent catalyst is responsible for both ethylene homopolymerization and styrene–ethylene copolymerization [38,80,81]. The observed formation of mixtures of homo- and copolymers is consistent with the presence of several active species in the polymerization medium. This latter point is now largely accepted and seems to be supported by some theoretical studies (*vide infra*).

7.2. Copolymerization mechanism

Only few mechanistic studies have been conducted with styrene–ethylene copolymerization catalytic systems. It is thus delicate to conclude on an accurate general mechanism from the features observed with specific systems. However, it seems reasonable to accept a predominant secondary regiochemistry of styrene insertion, as observed for sPS and in some cases for styrene–ethylene copolymerization [16,26,35], although the examination of the copolymer microstructure also reveals region-irregular styrene insertion.

The aforementioned discrepancies and controversies between authors about the microstructures of the copolymers (even when using the same catalytic system under close polymerization conditions) points out the fact that styrene–ethylene copolymerization mechanism with "single-site" catalysts is very complex and needs to be clarified.

For instance, Ishihara recently refuted Longo's results concerning the formation of block or alternated copolymers with titanium half-sandwich catalyst precursors [82]. Instead, the copolymers present styrene–styrene and ethylene–ethylene sequences. The latter are proposed to be formed through concomitant insertion of two ethylene molecules as depicted in Scheme 2.

7.3. Theoretical studies

Only very few publications, mainly from Martínez-Salazar and co-workers, have addressed styrene–ethylene copolymerization from a theoretical point of view [83–86].

In the case of the $CpTiCl_3$/MAO system, theoretical studies supported the tetravalent nature of the active species, stating that Ti^{III} gives rise to styrene homopolymers preferably. The mixture of homo- and copolymers observed experimentally was thus attributed to a $Ti^{IV} \rightarrow Ti^{III}$ reduction during polymerization. The prevalence of secondary styrene regiochemistry was also confirmed: after primary insertion, the phenyl ring strongly interacts with the metal center, blocking the active site in such a way that further polymerization is not possible ("dormant" species), while after secondary insertion, a free position is left so that polymerization can continue [83].

Metallocene catalysts *rac*-ethylenebis(tetrahydroindenyl) MCl_2 (M = Ti, Zr) were also examined by DFT [84,85]. Similarly, primary insertion of styrene leads to a dormant species with low propagation rate. The monomer insertion barriers were also much higher for the titanocene system than that of zirconocene, which is in agreement with the experimental observations (Zr systems more active than Ti systems [15]). A DFT study of the *meso* Zr isomer was also undertaken [86]. Unexpectedly, products formed after a first primary styrene insertion into *meso* catalyst can incorporate a new ethylene monomer and may continue the polymerization process, while the corresponding products from the *rac* isomer would lead to dormant species. This finding tends to indicate that higher styrene content could be achieved with *meso* complexes. Contrary to what is usually admitted for metallocene catalysts, some *meso* complexes were much more active than their *rac* counterparts for higher α-olefins (1-butene and 1-pentene) polymerization [87].

In contrast with metallocene catalysts, *secondary* insertion of styrene into Ti–CGC complexes would lead to dormant species. These could be reactivated by a further ethylene insertion [88]. In addition, complex with a more electron-rich indenyl ligand shows weaker coordination of the monomers and hence a slightly lower activity than its Cp analogue [89]. Surprisingly, when the co-catalyst was taken into account, the monomer coordination step was endothermic, both for ethylene and styrene, in contrast with values obtained for the naked cation. However, the global energetic insertion barriers starting from the π-complex were similar to those for the naked cation [90].

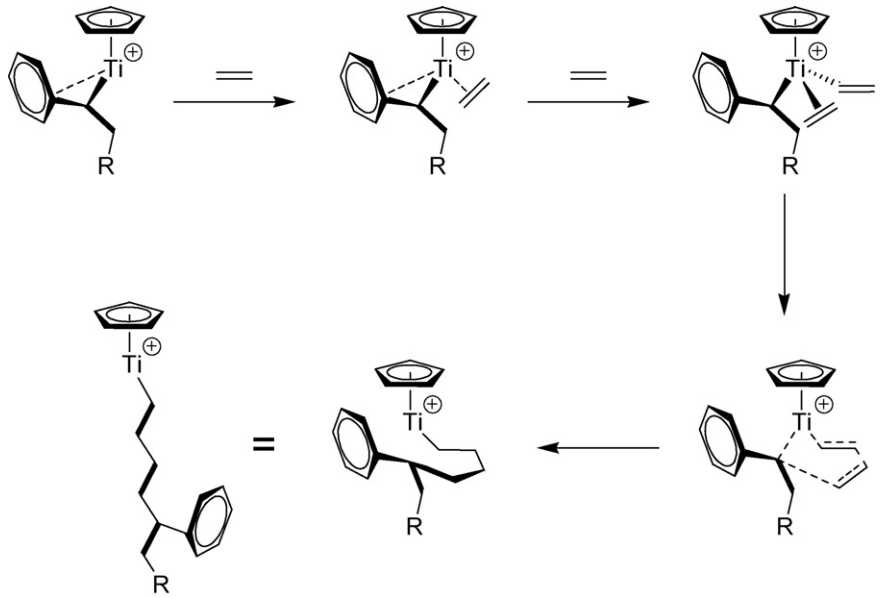

Scheme 2. Proposed mechanism for ethylene insertion with a titanium half-sandwich catalyst [82].

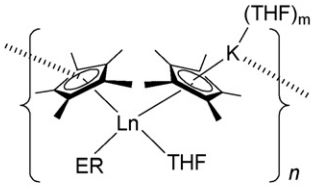

83-88 Ln = Sm ER = OAr^1, OAr^2, S-Ar^3, $HNAr^3$, $HPAr^4$, $N(SiMe_3)_2$
89-90 Ln = Sm ER = $CH(SiMe_3)_2$, SiH_3
91-92 Ln = Eu ER = $CH(SiMe_3)_2$, SiH_3
93-94 Ln = Yb ER = $CH(SiMe_3)_2$, SiH_3

Fig. 11. Divalent lanthanide half-sandwich complexes as single-component catalysts used for styrene–ethylene block copolymerization [91–93].

8. Group 3 catalysts

Styrene homo- and copolymerization mediated by group 3 catalysts has been much less explored than group 4 catalytic systems. Among the examples previously presented, only a few catalytic systems were reported to present some catalytic activity for styrene–ethylene copolymerization. These proved however to feature remarkable performances.

8.1. Lanthanide half-sandwich complexes

Divalent polymeric complexes **83–94** (Fig. 11) obtained by replacement of one of the Cp ligand in lanthanidocene by a monodentate anionic ligand (OAr, SAr, NR_1R_2 or SiR_3) yielded styrene–ethylene block copolymers in a one-step process under mild conditions (toluene, 25 °C, 1 atm) [91]. Homopolystyrene was formed as a by-product but no PE was detected. The selectivity for copolymerization rather than styrene homopolymerization depended on the ER ligand and the feeding amount of styrene: the thiolate complex **85** showed the highest selectivity (up to 96% copolymer) and formation of PS increased with the styrene feed. The incorporated styrene amount in the copolymer also increased almost linearly with rising the styrene feed. ^{13}C NMR and viscoelasticity analyses confirmed the blocky nature of the copolymers: these materials proved to be mechanically much stronger and more flexible than a mixture of homopolymers [92].

Sequential copolymerization experiments (styrene/styrene, styrene/ethylene and styrene/ethylene + styrene) strongly suggested that copolymerization is initiated by polymerization of ethylene and followed by successive incorporation of styrene. Reactions initiated by styrene polymerization afforded only PS, indicating that the propagation site in the system does not allow ethylene insertion, although it can generate a species (possibly a Sm^{III}-hydride) active for ethylene homopolymerization. The proposed mechanism for ER = aryloxide [92], thiolate [92], arylamide [92] and alkyl [93] complexes is depicted in Scheme 3.

In 2004, Hou and co-workers reported the efficient preparation of multiblock copolymers with highly syndiotactic styrenic sequences under mild conditions (toluene, 25 °C, 1 atm of ethylene) with the cationic scandium half-sandwich complex $[(C_5Me_4SiMe_3)Sc(CH_2SiMe_3)_2]^+ [B(C_6F_5)_4]^-$ (**95**, Scheme 4) [94]. The styrene content was easily controlled by styrene concentration in the feed and styrene-rich copolymers (up to 87 mol%) were obtained. Noteworthy and in striking contrast to many reports concerning styrene–ethylene copolymerization with other metal half-sandwich catalysts, no contamination by homopolymers (PE or PS) was observed. This represents one of the first regio- and stereoregular styrene copolymers reported. Furthermore, this catalytic system exhibits very high activities (up to 2314 kg sPS-*b*-PE/(mol_{Sc} h atm)) [94].

8.2. Ansa-lanthanidocene catalysts

The highest incorporated styrene contents in styrene–ethylene copolymers was achieved with the single-component allyl *ansa*-neodymocene catalyst (**96**, Scheme 5) reported by Carpentier and co-workers. This system yields poly(styrene-*co*-ethylene) composed of long syndiotactic polystyrene sequences connected by isolated ethylene units [95].

A detailed study showed that slightly higher polymerization activities are obtained in neat styrene but could lead to heat and mass transfer limitations due to very high viscosity of the polymerization medium. The temperature has a pronounced influence, though an increase in temperature did not give outstanding activities compared with other catalytic systems (maximal activity of 2529 kg P(S-*co*-E)/(mol_{Nd} h) for [St]/[Ln] = 1000 at 120 °C). However, those allyl *ansa*-lanthanidocene complexes proved to be stable up to 120 °C, which are industrially relevant conditions. The copolymers composition could be easily controlled by the monomer feeds over a wide range of composition, playing either with ethylene pressure and/or styrene concentration. The unusual higher affinity of those complexes towards styrene compared to ethylene was illustrated by the fact that no polymerization activity was detected at low styrene concentration (<1.2 mol/L) [95].

The effect of bulky substituents on the Cp moiety as well as the influence of the bridge atom were also investigated and revealed that this system is very sensitive to an increase in the steric bulkiness and that a non-hindered environment is crucial to achieve good catalytic performances [95].

The copolymer microstructure was assessed by ^{13}C NMR and further confirmed by TREF, DSC and DMA analyses which, unlike ESI copolymers, showed an increase in crystallinity, melting temperature T_m and glass transition temperature T_g with increasing styrene content [95].

The high syndiotacticity of the styrenic sequences observed in the copolymers led to a polymerization mechanism similar to that observed with those complexes for styrene homopolymerization, *i.e.* a prevailing chain-end mechanism along with a supposed contribution of an enantiomorphic site control.

8.3. Lanthanidocene catalysts with chain-transfer agents

In order to synthesize functionalized polymers, Marks efficiently coupled hydrosilylation and polymerization processes to yield polymers with silyl functional end-groups by using $PhSiH_3$ or nBuSiH_3 as chain-transfer agents and $[\{Me_2Si(C_5Me_4)_2\}LnH]_2$ (**97**, Ln = Nd, Sm) as catalysts [96].

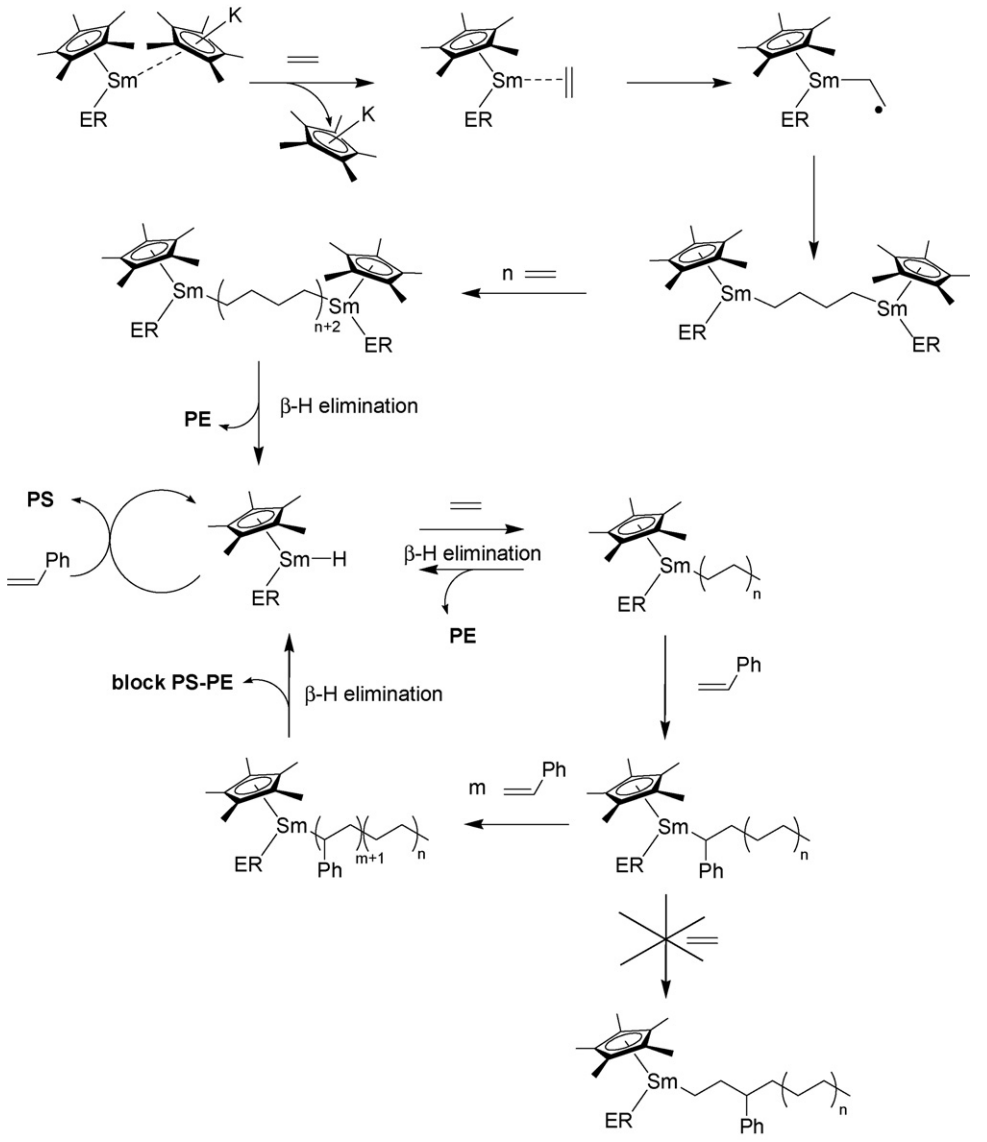

Scheme 3. Proposed mechanism for styrene–ethylene diblock copolymerization with divalent samarium half-sandwich catalysts [92].

The functionalized silapolyolefins thus obtained from styrene and ethylene present a random microstructure, with silyl groups delivered only to ethylene units, as determined by ^{1}H and ^{13}C NMR [97]. The recovered polymers showed low molecular weights (M_n = 1700–3300 g/mol, determined by ^{1}H NMR) and up to 26 mol% of incorporated styrene. The tacticity of the styrenic units was not mentioned. The global activities were quite low (3 kg/(mol$_{Ln}$ h)) but the copolymerization proceeded at room temperature. The proposed mechanism for this process is depicted in Scheme 6.

Reversible chain-transfer reactions between chlorolanthanidocenes and dialkylmagnesium compounds were also exploited to achieve styrene–ethylene block copolymers [98]. Indeed, complex $Cp^*_2NdCl_2Li(OEt_2)_2$ in combination with MgR_2, previously established as an efficient ethylene polymerization catalytic system [99–101], was also active for the formation of oligostyrenes. Thus, using a sequential procedure (either styrene polymerization followed by ethylene pressurization or ethylene polymerization followed by styrene introduction), atactic diblock copolymers formulated

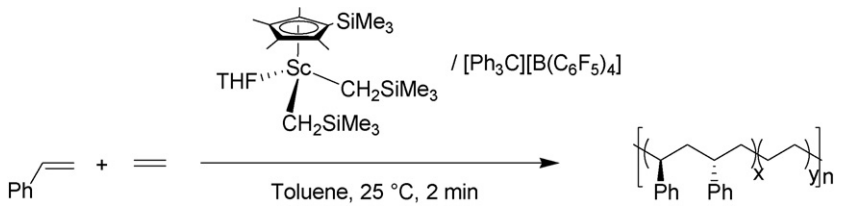

Scheme 4. Lanthanide half-sandwich catalytic system used for multiblock styrene–ethylene copolymerization [94].

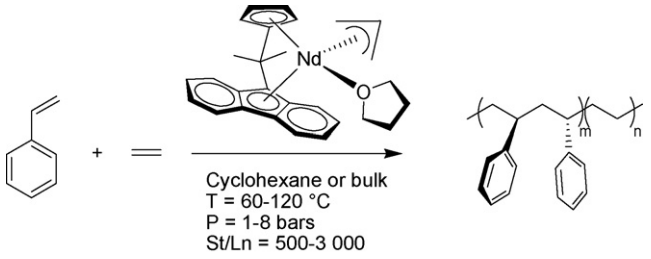

Scheme 5. Styrene–ethylene copolymerization catalyzed by allyl *ansa*-neodymocene [95].

as $[CH_2CH(Ph)]_x - [CH_2CH_2]_y$ with $x = 10$–13 and $y = 3$–20 (corresponding to 38–65 mol% styrene incorporation) were synthesized [98].

9. Copolymerization of styrene with α-olefins

9.1. Styrene–propylene copolymerization

Similar to the copolymerization of styrene with ethylene, styrene–propylene copolymerization by heterogeneous Ziegler–Natta catalysts (for instance $TiCl_3/AlEt_3$) leads to mixtures of PP, PS and some propylene-rich copolymer [102]. Styrene–propylene copolymerization mediated by homogeneous single-site catalysts was generally achieved with the same type of complexes than the ones active for styrene–ethylene copolymerization. However, due to the opposite insertion regiospecificities of styrene and propylene, only a few efficient examples have quite recently appeared in the literature.

9.1.1. Metallocene catalysts

As presented above in Section 3, some observations suggested that styrene insertion in styrene–ethylene copolymerization occurs in a secondary fashion with *ansa*-metallocene-based catalysts. On the other hand, the primary insertion of propylene is now widely accepted with those catalysts. As a consequence, steric hindrance would prevent both primary propylene and secondary styrene insertions into the metal–polymer bond when the last inserted unit is a secondary styrene (it was observed that styrene–styrene sequences are forbidden). Oliva and coworkers elegantly achieved the goal of introducing some styrene units into isotactic PP in order to confer new properties to the material by adding small amounts of ethylene with the idea that traces of this third monomer could reactivate the catalytic site produced from complex *rac*-(EBI)$ZrCl_2$ (**9**) after secondary styrene insertion [103]. Despite the presence of three

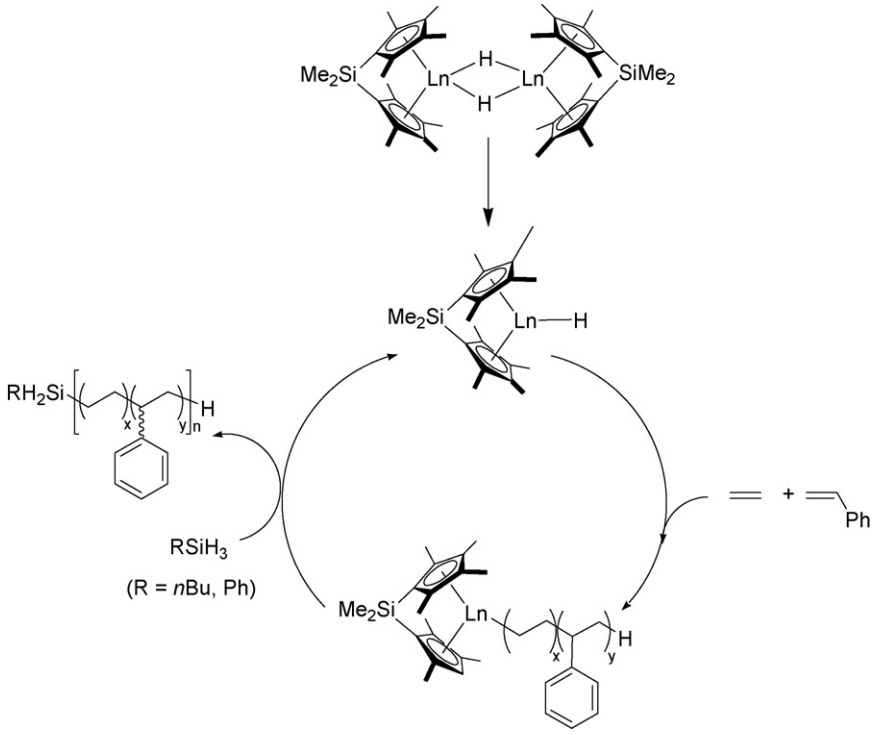

Scheme 6. Proposed catalytic cycle for silyl end-capped polyolefins synthesis catalyzed by organolanthanide catalysts [96].

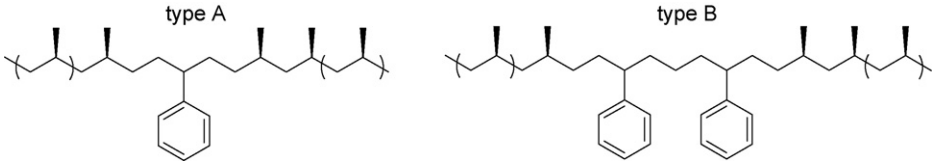

Fig. 12. Observed monomer sequences incorporated in *i*PP with complex **9** [103].

different monomers, only two different repeating units could be detected in the copolymer chain: ethylene was inserted only after styrene insertion and no PEP sequences could be distinguished (Fig. 12).

A similar insertion behavior and copolymer microstructure was observed with C_s-symmetric catalyst precursor ($C_5H_4CMe_2Flu$)$ZrCl_2$ (**1**) but with syndiotactic polypropylene sequences instead of isotactic ones [104]. The stereoselectivity of the secondary styrene insertion with both C_2 and C_s catalysts was also determined by ^{13}C NMR of the copolymers prepared with ^{13}C-enriched ethylene. The (*R*,*R*) C_2-symmetric catalyst prefers *S*-styrene insertion, while with the C_s-catalyst, the *R*-enantioface is preferred at the *R*-catalytic site [104].

The structural characterization of the polymer obtained with the C_s catalyst showed that styrene–ethylene units are segregated in the amorphous phase and that the bulky styrene monomer prevents the inclusion of ethylene in the sPP crystal lattice, hence minimizing the influence on PP polymorphism [105].

9.1.2. Titanium half-sandwich catalysts

Block copolymerization of styrene and propylene was also achieved through a sequential protocol using the catalytic system Cp*Ti(OBz)$_3$/MAO [106]. When both monomers were injected at the same time, only sPS was recovered. However, when propylene was first pre-polymerized by Cp*Ti(OBz)$_3$/MAO, and styrene and TIBA were then added, the copolymerization product was a mixture of some homopolymers and block styrene–propylene copolymer that was separated by fractionation. Consistent with the microstructures found for respective homopolymerizations with this catalyst, ^{13}C NMR analyses indicated that the PS segments present a syndiotactic configuration while the PP sequences were atactic. Opposite to the results observed in styrene–ethylene copolymerization, the propene content in the copolymer was quite low (20 mol%), leading to a material that presented rubbery phases along with crystalline regions and hence a better toughness and improved impact strength compared to sPS [107].

9.1.3. Constrained geometry catalysts

Strangely enough, no constrained geometry complexes were reported in the literature for styrene–propylene copolymerization except for one recent example [108]. The CGC systems (3,6-*t*BuFluSiMe$_2$N*t*Bu)TiX$_2$/MAO (X = Cl, Me) (**98**–**99**, Fig. 13) have been investigated in copolymerization of propylene with styrene under relatively mild conditions (25–60 °C, 1–5 atm, 500 equiv. of MAO) and gave random styrene–propylene copolymers with up to 24 mol% incorporated styrene and moderate molecular weights (M_n = 14,000–88,000 g/mol; M_w/M_n = 1.6–2.3). The microstructure determined by ^{13}C NMR revealed predominant syndiotactic polypropylene sequences and randomly distributed single styrenic units and/or very short polystyrene sequences. Similar to the observations made by Oliva, the introduction of small ethylene amounts as a co-monomer significantly enhances polymerization activity, without notable impact on the molecular weight, polydispersity and microstructure of the copolymers [108].

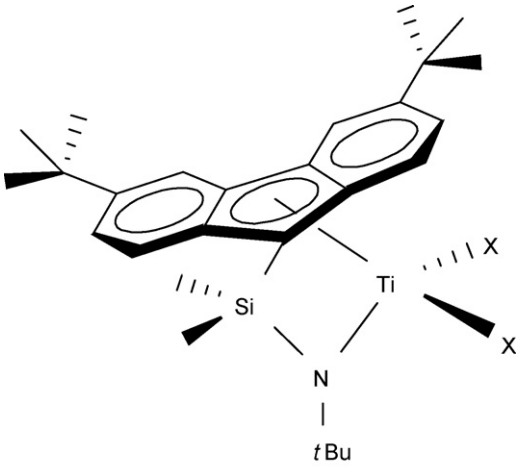

98-99 X = Cl, Me

Fig. 13. Constrained geometry catalyst precursors used for styrene–propylene copolymerization [108].

9.1.4. Bis(phenolate) catalysts

The post-metallocene complex **100** (Fig. 14), which was previously reported to promote styrene–ethylene copolymerization [70–74] (*vide supra*), could also oligomerize propylene upon MAO-activation to give oligomers presenting predominantly unsaturated chain-ends that are diagnostic of a primary insertion regiochemistry [109].

In the presence of styrene, propylene polymerization by **100**, activated by 500 equiv. of MAO, produced multiblock copolymers containing long isotactic styrene sequence interrupted by short isotactic propylene sequences (average of five units enchained in a primary fashion) [109]. ^{13}C NMR analysis of the polymer showed that the opposite regiochemistry of the two monomers was retained, producing tail-to-tail (secondary styrene insertion followed by primary propylene insertion) and head-to-head (primary propylene insertion followed by secondary styrene insertion) linkages between the homopolymers blocks, as depicted in Fig. 15. The thermal behavior confirmed the multiblock nature: the presence of propylene in the polymer chain reduced the melting temperature with respect to *i*PS.

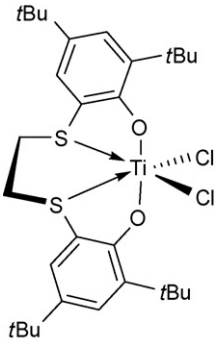

100

Fig. 14. OSSO titanium catalyst precursor used for styrene–propylene copolymerization [109].

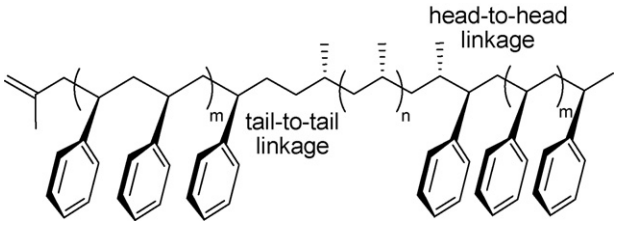

Fig. 15. Detailed microstructure of styrene–propylene multiblock copolymers produced with **100**/MAO [109].

9.2. Copolymerization of styrene with higher α-olefins

9.2.1. Styrene–hexene copolymerization

The copolymerization of styrene with α-olefins higher than propylene remains very rare, probably due to the modest performances obtained with the latter monomer. Recently, copolymerization of styrene and 1-hexene with the homogeneous and silica-supported systems based on *rac*-(EBI)$ZrCl_2$/MAO (**9**) was claimed [110]. Consistent with the higher homopolymerization activity observed toward 1-hexene than toward styrene, the amount of incorporated hexene was higher than that of styrene relative to the initial monomer feed (up to 54 mol% incorporated styrene for a molar ratio [styrene]/[hexene] = 3 in the feed). Also in agreement with the selectivity previously observed, the system gave isotactic hexene sequences but atactic styrene ones.

9.2.2. Styrene–1-alkene copolymerization

The same system, used with the addition of Ph_2Zn, was also effective for styrene copolymerization with 1-octene, 1-decene, 1-dodecene, 1-hexadecene and 1-octadecene [111–113]. A further contribution stated that this initiator system gave isotactic olefin-enriched copolymers, with a poorer styrene incorporation than that of 1-alkene (up to 65 mol% for a feed ratio [styrene]/[alkene] = 3). According to DSC analyses, the copolymers are crystalline, featuring a melting temperature $T_m \approx 40\,^{\circ}C$ [114].

However, no blank experiment without Ph_2Zn was carried out to determine the exact role of the diphenylzinc in the initiation step. The latter was simply assumed to behave as a Lewis acid, favoring the reduction of the metal center. On the other hand, a mixture of the latter and MAO could produce some polymers (probably atactic PS) under the conditions used. Thus, those results arouse some doubts concerning their accuracy.

10. Concluding remarks

Many efforts have been paid to improve the brittleness and high melting temperature of sPS – which constitute major limitations from an industrial point of view – by introducing another monomer in the polystyrene chain *via* copolymerization protocols. However, many of the traditional catalytic systems able to produce PE and/or sPS that have been assessed in styrene–ethylene copolymerization afforded generally atactic random or alternating microstructures, overall poor performances and often mixtures of homopolymers. Successful examples of systems enabling a substantial control of monomers incorporation remain rare, as well as the most desired styrene-rich copolymers. This is often due to better catalyst reactivity towards ethylene monomer than towards styrene. Current challenges in this chemistry invoke therefore the design of catalysts that feature a *single-site* behavior *and* at least equal reactivity towards styrene than with ethylene. Considering the fundamental differences in the reactivity of these two monomers with metal complexes, this is obviously a difficult task, but discrete group 3 catalysts have recently shown promises in this direction.

References

[1] K. Soga, D.-H. Lee, H. Yanagihara, Polym. Bull. 20 (1988) 237.
[2] R. Mani, C.M. Burns, Macromolecules 24 (1991) 5476.
[3] N. Niessner, H. Gausepohl, in: D.J. Scheirs, D.B. Priddy (Eds.), Modern Styrenic Polymers: Polystyrenes and Styrenic Copolymers, Wiley & Sons, 2003, p. 25.
[4] C. Pellecchia, L. Oliva, Rubber Chem. Technol. 72 (1999) 553.
[5] P.S. Chum, W.J. Kruper, M.J. Guest, Adv. Mater. 12 (2000) 1759.
[6] H. Chen, M.J. Guest, S. Chum, A. Hiltner, E. Baer, J. Appl. Polym. Sci. 70 (1998) 109.
[7] H.Y. Chen, E.V. Stepanov, S.P. Chum, A. Hiltner, E. Baer, Macromolecules 32 (1999) 7587.
[8] H.Y. Chen, E.V. Stepanov, S.P. Chum, A. Hiltner, E. Baer, J. Polym. Sci., Part B: Polym. Phys. 37 (1999) 2373.
[9] Y.W. Cheung, M.J. Guest, J. Polym. Sci., Part B: Polym. Phys. 38 (2000) 2976.
[10] Y.W. Cheung, M.J. Guest, in: D.J. Scheirs, D.B. Priddy (Eds.), Modern Styrenic Polymers: Polystyrenes and Styrenic Copolymers, Wiley & Sons, 2003, p. 605.
[11] J.C. Randall, J. Macromol. Sci., Part C: Rev. Macromol. Chem. Phys. 29 (1989) 201.
[12] J. Ren, G.R. Hatfield, Macromolecules 28 (1995) 2588.
[13] I. Albers, W. Kaminsky, U. Weingarten, R. Werner, Catal. Commun. 3 (2002) 105.
[14] W. Kaminsky, I. Albers, M. Vathauer, Des. Monomers Polym. 5 (2002) 155.
[15] N. Haider, M.T. Expósito, A. Muñoz-Escalona, J. Ramos, J.F. Vega, L. Méndez, J. Martínez-Salazar, J. Appl. Polym. Sci. 102 (2006) 3420.
[16] L. Oliva, L. Caporaso, C. Pellecchia, A. Zambelli, Macromolecules 28 (1995) 4665.
[17] L. Oliva, L. Izzo, P. Longo, Macromol. Rapid Commun. 17 (1996) 745.
[18] V. Venditto, G. De Tullio, L. Izzo, L. Oliva, Macromolecules 31 (1998) 4027.
[19] T. Suzuki, Y. Tsuji, Y. Watanabe, Y. Takegami, Macromolecules 13 (1980) 849.
[20] L. Izzo, L. Oliva, A. Proto, M. Trofa, Macromol. Chem. Phys. 200 (1999) 1086.
[21] L. Oliva, A. Immirzi, C. Tedesco, V. Venditto, A. Proto, Macromolecules 32 (1999) 2675.
[22] L. Oliva, P. Longo, L. Izzo, M. Di Serio, Macromolecules 30 (1997) 5616.
[23] T. Arai, T. Ohtsu, S. Suzuki, Polym. Prepr. 39 (1998) 220.
[24] T. Arai, T. Ohtsu, S. Suzuki, Macromol. Rapid Commun. 19 (1998) 327.
[25] L. Caporaso, L. Izzo, I. Sisti, L. Oliva, Macromolecules 35 (2002) 4866.
[26] L. Izzo, M. Napoli, L. Oliva, Macromolecules 36 (2003) 9340.
[27] M. Lobon-Poo, J.O. Barcina, A.G. Martinez, M.T. Exposito, J.F. Vega, J. Martinez-Salazar, M.L. Reyes, Macromolecules 39 (2006) 7479.
[28] A. Grassi, M. Caprio, A. Zambelli, D.E. Bowen, Macromolecules 33 (2000) 8130.
[29] P. Longo, A. Grassi, L. Oliva, Makromol. Chem. 191 (1990) 2387.
[30] P. Aaltonen, J. Seppala, Eur. Polym. J. 30 (1994) 683.
[31] P. Aaltonen, J. Seppala, Eur. Polym. J. 31 (1995) 79.
[32] L. Oliva, S. Mazza, P. Longo, Macromol. Chem. Phys. 197 (1996) 3115.
[33] P.P. Chu, H.S. Tseng, Y.P. Chen, D.D. Yu, Polymer 41 (2000) 8271.
[34] C. Pellecchia, D. Pappalardo, M. D'Arco, A. Zambelli, Macromolecules 29 (1996) 1158.

[35] A. Zambelli, C. Pellecchia, L. Oliva, P. Longo, A. Grassi, Makromol. Chem. 192 (1991) 223.
[36] C. Pellecchia, M. Mazzeo, G.-J. Gruter, Macromol. Rapid Commun. 20 (1999) 337.
[37] C. Pellecchia, D. Pappalardo, L. Oliva, M. Mazzeo, G.-J. Gruter, Macromolecules 33 (2000) 2807.
[38] G. Xu, S. Lin, Macromolecules 30 (1997) 685.
[39] Q. Wu, Z. Ye, Q. Gao, S. Lin, Macromol. Chem. Phys. 199 (1998) 1715.
[40] F. Zhu, Y. Fang, S. Lin, J. Appl. Polym. Sci. 74 (1999) 1851.
[41] K. Nomura, T. Komatsu, Y. Imanishi, Macromolecules 33 (2000) 8122.
[42] K. Nomura, H. Okumura, T. Komatsu, N. Naga, Macromolecules 35 (2002) 5388.
[43] H. Zhang, D.J. Byun, K. Nomura, Dalton Trans. (2007) 1802.
[44] H. Zhang, K. Nomura, J. Am. Chem. Soc. 127 (2005) 9364.
[45] H. Zhang, K. Nomura, Macromolecules 39 (2006) 5266.
[46] T. Ishiyama, K. Miyoshi, H. Nakazawa, J. Mol. Catal. A: Chem. 221 (2004) 41.
[47] A.L. McKnight, R.M. Waymouth, Chem. Rev. 98 (1998) 2587.
[48] H. Braunschweig, F.M. Breitling, Coord. Chem. Rev. 250 (2006) 2691.
[49] P.J. Shapiro, E. Bunel, W.P. Schaefer, J.E. Bercaw, Organometallics 9 (1990) 867.
[50] P.J. Shapiro, W.P. Schaefer, J.A. Labinger, J.E. Bercaw, W.D. Cotter, J. Am. Chem. Soc. 116 (1994) 4623.
[51] J. Okuda, Chem. Ber. 123 (1990) 1649.
[52] J. Okuda, F.J. Schattenmann, S. Wocadlo, W. Massa, Organometallics 14 (1995) 789.
[53] J.C. Stevens, F.J. Timmers, D.R. Wilson, G.F. Schmidt, P.N. Nickias, R.K. Rosen, G.W. Knight, Dow Chemical Company, EP 0,416,815 A2 (1991).
[54] J.A.M. Canich, Exxon Chemical, US Patent 5,026,798 (1991).
[55] D.J. Arriola, M. Bokota, R.E. Campbell, J. Klosin, R.E. LaPointe, O.D. Redwine, R.B. Shankar, F.J. Timmers, K.A. Abboud, J. Am. Chem. Soc. 129 (2007) 7065.
[56] F.G. Sernetz, R. Mülhaupt, R.M. Waymouth, Macromol. Chem. Phys. 197 (1996) 1071.
[57] F.G. Sernetz, R. Mülhaupt, F. Amor, T. Eberle, J. Okuda, J. Polym. Sci., Part A: Polym. Chem. 35 (1997) 1571.
[58] G. Xu, Macromolecules 31 (1998) 2395.
[59] T.A. Sukhova, A.N. Panin, O.N. Babkina, N.M. Bravaya, J. Polym. Sci., Part A: Polym. Chem. 37 (1999) 1083.
[60] R. Skeril, P. Sindelar, Z. Salajka, V. Varga, I. Cisarova, J. Pinkas, M. Horacek, K. Mach, J. Mol. Catal. A: Chem. 224 (2004) 97.
[61] S. Gentil, N. Pirio, P. Meunier, F. Gallou, L.A. Paquette, Eur. Polym. J. 40 (2004) 2241.
[62] M. Kamigaito, T.K. Lal, R.M. Waymouth, J. Polym. Sci., Part A: Polym. Chem. 38 (2000) 4649.
[63] K. Nomura, H. Okumura, T. Komatsu, N. Naga, Y. Imanishi, J. Mol. Catal. A: Chem. 190 (2002) 225.
[64] M. Fineman, S.D. Ross, J. Polym. Sci. 5 (1950) 259.
[65] J.A. Ewen, R.L. Jones, A. Razavi, J.D. Ferrara, J. Am. Chem. Soc. 110 (1988) 6255.
[66] M.A. Giardello, M.S. Eisen, C.L. Stern, T.J. Marks, J. Am. Chem. Soc. 117 (1995) 12114.
[67] G. Odian, Principles of Polymerization, fourth edition, 2004, pp. 464.
[68] N. Guo, L. Li, T.J. Marks, J. Am. Chem. Soc. 126 (2004) 6542.
[69] S.K. Noh, J. Lee, D.-H. Lee, J. Organomet. Chem. 667 (2003) 53.
[70] M. Kakugo, T. Miyatake, K. Mizunuma, Stud. Surf. Sci. Catal. 56 (1990) 517.
[71] M. Kakugo, T. Miyatake, K. Mizunuma, Y. Yagi, Sumitomo, US 5,043,408 (1991).
[72] T. Miyatake, K. Mizunuma, M. Kakugo, Macromol. Symp. 66 (1993) 203.
[73] S. Fokken, T.P. Spaniol, J. Okuda, F.G. Sernetz, R. Mulhaupt, Organometallics 16 (1997) 4240.
[74] F.G. Sernetz, R. Mulhaupt, S. Fokken, J. Okuda, Macromolecules 30 (1997) 1562.
[75] J.C.W. Chien, Z. Salajka, J. Polym. Sci., Part A: Polym. Chem. 29 (1991) 1243.
[76] J.C.W. Chien, Z. Salajka, S. Dong, Macromolecules 25 (1992) 3199.
[77] C. Capacchione, A. Proto, H. Ebeling, R. Mülhaupt, J. Okuda, J. Polym. Sci., Part A: Polym. Chem. 44 (2006) 1908.
[78] C. Capacchione, M. D'Acunzi, O. Motta, L. Oliva, A. Proto, J. Okuda, Macromol. Chem. Phys. 205 (2004) 370.
[79] M.-S. Weiser, R. Mülhaupt, Macromol. Rapid Commun. 27 (2006) 1009.
[80] A. Grassi, A. Zambelli, F. Laschi, Organometallics 15 (1996) 480.
[81] R.J. Maldanis, J.C.W. Chien, M.D. Rausch, J. Organomet. Chem. 599 (2000) 107.
[82] K. Yokota, T. Kohsaka, K. Ito, N. Ishihara, J. Polym. Sci., Part A: Polym. Chem. 43 (2005) 5041.
[83] A. Munoz-Escalona, V. Cruz, N. Mena, S. Martinez, J. Martinez-Salazar, Polymer 43 (2002) 7017.
[84] S. Martinez, V. Cruz, A. Munoz-Escalona, J. Martinez-Salazar, Polymer 44 (2003) 295.
[85] M.T. Exposito, S. Martinez, J. Ramos, V. Cruz, M. Lopez, A. Munoz-Escalona, N. Haider, J. Martinez-Salazar, Polymer 45 (2004) 9029.
[86] S. Martínez, J. Ramos, V.L. Cruz, J. Martínez-Salazar, J. Polym. Sci., Part A: Polym. Chem. 44 (2006) 4752.
[87] M. Vathauer, W. Kaminsky, Macromolecules 33 (2000) 1955.
[88] S. Martínez, M.T. Exposito, J. Ramos, V. Cruz, M.C. Martínez, M. López, A. Muñoz-Escalona, J. Martínez-Salazar, J. Polym. Sci., Part A: Polym. Chem. 43 (2005) 711.
[89] S.H. Yang, W.H. Jo, S.K. Noh, J. Chem. Phys. 119 (2003) 1824.
[90] S. Martinez, J. Ramos, V.L. Cruz, J. Martinez-Salazar, Polymer 47 (2006) 883.
[91] Z. Hou, H. Tezuka, Y. Zhang, H. Yamazaki, Y. Wakatsuki, Macromolecules 31 (1998) 8650.
[92] Z. Hou, Y. Zhang, H. Tezuka, P. Xie, O. Tardif, T.-A. Koizumi, H. Yamazaki, Y. Wakatsuki, J. Am. Chem. Soc. 122 (2000) 10533.
[93] Z. Hou, Y. Zhang, M. Nishiura, Y. Wakatsuki, Organometallics 22 (2003) 129.
[94] Y. Luo, J. Baldamus, Z. Hou, J. Am. Chem. Soc. 126 (2004) 13910.
[95] A.-S. Rodrigues, E. Kirillov, C.W. Lehmann, T. Roisnel, B. Vuillemin, A. Razavi, J.-F. Carpentier, Chem. Eur. J. 13 (2007) 5548.
[96] P.-F. Fu, T.J. Marks, J. Am. Chem. Soc. 117 (1995) 10747.
[97] K. Koo, P.-F. Fu, T.J. Marks, Macromolecules 32 (1999) 981.
[98] S. Bogaert, J.-F. Carpentier, T. Chenal, A. Mortreux, G. Ricart, Macromol. Chem. Phys. 201 (2000) 1813.
[99] T.M. Petitjohn, Phillips Petroleum, US Patent 5,109,085 (1992).
[100] X. Olonde, A. Mortreux, F. Petit, K. Bujadoux, J. Mol. Catal. 82 (1993) 75.
[101] J.-F. Pelletier, A. Mortreux, X. Olonde, K. Bujadoux, Angew. Chem. Int. Ed. 35 (1996) 1854.
[102] K. Soga, H. Yanagihara, Macromolecules 22 (1989) 2875.
[103] L. Caporaso, L. Izzo, L. Oliva, Macromolecules 32 (1999) 7329.
[104] L. Caporaso, L. Izzo, S. Zappile, L. Oliva, Macromolecules 33 (2000) 7275.
[105] C. De Rosa, A. Buono, L. Caporaso, L. Oliva, Macromolecules 36 (2003) 7119.
[106] S. Lin, Q. Wu, R. Chen, F. Zhu, Macromol. Symp. 195 (2003) 63.
[107] R. Chen, Q. Wu, F. Zhu, S. Lin, J. Appl. Polym. Sci. 89 (2003) 1596.
[108] E. Kirillov, A. Razavi, J.-F. Carpentier, J. Mol. Catal. A: Chem. 249 (2006) 230.
[109] C. Capacchione, F. DeCarlo, C. Zannoni, J. Okuda, A. Proto, Macromolecules 37 (2004) 8918.
[110] S. Rahmani, M. Abbasian, P.N. Moghadam, A.A. Entezami, J. Appl. Polym. Sci. 104 (2007) 4008.
[111] F.M. Rabagliati, M.A. Pérez, R.A. Cancino, M.A. Soto, F.J. Rodríguez, C.J. Caro, A.G. León, H.A. Ayal, R. Quijada, Macromol. Symp. 168 (2001) 31.
[112] F.M. Rabagliati, M.A. Pérez, R.A. Cancino, F.J. Rodríguez, C.J. Caro, Macromol. Symp. 195 (2003) 81.
[113] F.M. Rabagliati, R.A. Cancino, M.A. Pérez, F.J. Rodríguez, Macromol. Symp. 216 (2004) 55.
[114] F.M. Rabagliati, R.A. Cancino, A. Martinez de Ilarduya, S. Munoz-Guerra, Eur. Polym. J. 41 (2005) 1013.